PCCP

Electronic spectra of linear isoelectronic species HC_6H^+, C_6H, HC_5N^+

Zexing Cao[ab] **and Sigrid D. Peyerimhoff** *[a]

[a] *Institut für Physikalische und Theoretische Chemie, Universität Bonn, Wegelerstrasse 12, D-53115 Bonn, Germany. E-mail: unt000@uni-bonn.de*
[b] *Department of Chemistry, State Key Laboratory for Physical Chemistry of the Solid Surface, Xiamen University, Xiamen 361005, China*

Multireference configuration interaction calculations have been used to determine term energies of low-lying doublet electronic states of isoelectronic carbon chains HC_6H^+, C_6H and HC_5N^+. Calculations on relevant excited states in the energy range up to 6 eV show that $^2\Pi$ and $^2\Phi$ excited states due to the π–π excitation are comparable in energy pattern among such species, but that there are significant differences in the properties of $^2\Sigma$ and $^2\Delta$ excited state series of these isoelectronic species. Similarities and discrepancies are discussed based on molecular orbital energy patterns and electron correlation. The strongest transitions for HC_6H^+, C_6H and HC_5N^+ are predicted to correspond to $X\,^2\Pi \to 2\,^2\Pi$ transitions at 2.22, 2.56 and 2.17 eV, respectively. For HC_6H^+, no $^2\Sigma$ or $^2\Delta$ states arising from σ–π electron promotion are found in the energy range up to 6 eV. However, in C_6H the first excited state $1\,^2\Sigma^+$ due to the $13\sigma \to 3\pi$ excitation is found to be only slightly higher (0.22 eV) than the ground state $X\,^2\Pi$. Calculated transition energies in the present study show good agreement with available experimental results.

Introduction

Polyacetylene and cyanopolyacetylene linear chains and their derivatives are important relatives of the carbon cluster family because of their importance in chemical processes[1] and in interstellar environments.[2–4] The electronic spectra of a variety of such chains have been identified by matrix isolation spectroscopy.[5–8] These observations give a thorough understanding of the electronic structure of such species in their ground and in some excited states and a profound discussion of the possible relevance of carbon chains as carriers of the diffuse interstellar bands (DIBs).

Polyacetylene cations, HC_nH^+ with the even-numbered n, and the isoelectronic chains, C_nH, as well as cyanopolyacetylene cations, $HC_{n-1}N^+$, have an $X\,^2\Pi$ ground state arising from a π^3 configuration. $X\,^2\Pi$–$^2\Pi$ electronic transitions due to the π–π electron promotion in these isoelectronic species have strong absorptions in the region of the observed DIBs, *i.e.* in the 400–900 nm region.[5] For example, when we compare isoelectronic species, *e.g.* HC_6H^+, HC_5N^+ and C_6H, their $A\,^2\Pi \leftarrow X\,^2\Pi$ electronic transitions occur at 605, 584 and 530 nm, respectively. Further, the wavelength of the strongest band origin of the π–π electronic transition of the polyacetylene series shows an approximate linear dependence on the number of carbon atoms in the odd-numbered $HC_{2n+1}H^+$ and even-numbered $HC_{2n}H^+$ chain, respectively.

Although the lowest transitions due to π–π electron excitations in these chains are relatively well characterized experimentally, higher $X\,^2\Pi$–$^2\Pi$ transitions observed beyond the $X\,^2\Pi \to A\,^2\Pi$ band are still not well understood.[5] Further assignments of the observed bands require reliable theoretical knowledge of the low-lying electronic states. In order to get insight into the electronic spectra of such carbon chains observed in matrix isolation spectroscopy, extensive theoretical calculations on representative isoelectronic species HC_6H^+, HC_5N^+ and C_6H, are performed in the present work. Structures, vibrational frequencies, and electronic spectra of these species are investigated by density functional theory (DFT) and sophisticated *ab initio* methodologies.

Computational details

DFT calculations with the B3LYP functional[9,10] were used to determine the equilibrium geometries and vibrational frequencies of the molecules in their ground states. For comparison, geometry optimizations of these species have also been performed by MP2 and CISD calculations with the 6-311G*[11,12] basis set and by the RCCSD method with the polarized triplet-zeta basis set.[13] These calculations were carried out with GAUSSIAN 94[14] and MOLPRO 97[15] programs, respectively.

Electronic transition energies were calculated by the multireference configuration interaction procedure (MRCI) implemented in the new DIESEL program.[16] The oscillator strengths are computed with the length gauge. Generally these values are more stable with respect to possible deficiencies in the wavefunction than the results from the velocity gauge. The AO basis set employed in the MRCI calculation is the 9s5p/5s3p[17] gaussian set plus an additional d polarization function with an exponent of 0.75 for all C and N atoms. This basis set is fairly flexible to describe both the ground and excited states in a balanced treatment. For all H atoms, a standard 3-21G basis set is employed in this study. In the MRCI calculation, 21 valence electrons are involved in the active reference space, while the core and the lowest 2 valence orbitals are always kept double occupied. Previous calculations show that this treatment is sufficient to obtain the electronic spectra.[18] The configuration selection threshold was generally $10^{-6}\,E_h$. The effect of higher than double excitations on electron correlation was estimated by a generalized Davidson procedure,[19] *i.e.*

$$E = [(1 - c_0^2)/c_0^2][E_{\text{MRD-CI}} - E_{\text{ref CI}}],$$

where c_0^2 is the contribution of the reference configurations to the total CI wavefuction and $E_{\text{MRD-CI}}$ and $E_{\text{ref CI}}$ correspond to the energies of the multireference single and double excitation and the reference CI, respectively. This extrapolated full CI limit with Davidson's correction will be used throughout in the present study. Usually, the Davidson correction may lower the transition energy by 0.1–0.2 eV (*vide infra*) in comparison with the extrapolated MRD-CI alone.

The RCCSD optimized geometry of HC_6H^+ in its ground state, the RCCSD(T) optimized geometry of C_6H from ref 20, and the B3LYP optimized geometry of HC_5N^+ are used in the MRD-CI calculation.

Results and discussion

Geometries and vibrational frequencies

The optimized bond lengths of isoelectronic species HC_6H^+, C_6H and HC_5N^+ at several levels of theory are shown in Fig. 1. The separations among the carbon atoms suggest a dominant acetylene bonding character in these species, *e.g.* an H–C≡C–C≡C–C≡C–H$^+$ structure for HC_6H^+. A comparison of B3LYP optimized bond lengths with sophisticated RCCSD and RCCSD(T)[20a] treatments shows that B3LYP calculations predict excellent geometries. The calculated rotation constants of 0.044 672, 0.046 365, 0.044 778 cm^{-1} for HC_6H^+, C_6H and HC_5N^+ in their ground states, respectively, are in reasonable agreement with corresponding experimental values of 0.044 594 3,[20b] 0.046 404 9,[20c] 0.044 616 5 cm^{-1}.[20d] Harmonic vibrational frequencies of these species in their ground states by B3LYP calculations are presented in Table 1. Inspection of B3LYP vibrational analyses in Table 1 shows good agreement with available experimental fundamentals.[7,8,21,22] This reliable performance of B3LYP calculations for the structure of

carbon clusters has been seen in previous theoretical studies.[23-25]

Electronic structures

The isoelectronic species HC_6H^+, C_6H and HC_5N^+ have a similar electron configuration $\ldots 2\pi^4\, 3\pi^3$ (in $C_{\infty v}$ notation). The relative energies of molecular orbitals (MOs) of these isoelectronic chains are displayed in Fig. 2. These MO energy levels show a similar pattern for the π MOs while significant distinctions are seen in the σ MO series. In particular, the $7\sigma_g$ and $6\sigma_u$ are almost degenerate in HC_6H^+, as in C_6 (*vide infra*), while notable splittings occur between corresponding 13σ and 12σ MOs in the systems C_6H and HC_5N^+.

In comparison with the neutral species C_6H, the general shift of MO energy levels to lower energies in HC_6H^+ and HC_5N^+ is due to the positive charge. The significant change in the ordering of σ MOs relative to those of π symmetry from C_6 to C_6H and HC_6H^+ results from admixture of hydrogen atomic orbitals (AOs). In HC_6H^+ both orbitals, $6\sigma_u$ and $7\sigma_g$, which are almost isoenergetic in C_6, are stabilized by mixing with the hydrogen obitals. Such stabilization is also present in comparing orbital energies of C_2 with those of C_2H_2 and C_2H_4.[26] In C_6H, on the other hand, only one hydrogen AO is available for mixing with the parent $6\sigma_u$ and $7\sigma_g$; furthermore, because of the loss of gerade and ungerade symmetry 13σ ($7\sigma_g$) and 12σ ($6\sigma_u$) can interact. As a result, the 13σ in C_6H is located in the energy region of frontier π MOs, comprising a more complex MO pattern than that in HC_6H^+. These interactions arising from these orbitals are shown in Fig. 3 (where the electron from hydrogen, entering into the HOMO π, is omitted). The situation in HC_5N^+ is, in principle, similar to that in HC_6H^+ because at one terminal of the C_6-like chain the $6\sigma_u$, $7\sigma_g$-type orbitals are stabilized due to hydrogen mixing and at the other terminal position they are stabilized due to the higher nuclear charge of nitrogen relative to carbon. Because of the lower symmetry, these two orbitals interact, so that a large splitting between the respective orbital energies of 12σ and 13σ is observed, unlike in HC_6H^+; nevertheless it is considerably smaller than that in C_6H. Similarities in π MO patterns and differences in σ MO systems shown in Fig. 2 are expected to account for different features of electronic spectra due to π and σ electron promotion, respectively, for these isoelectronic species.

Energies of doublet states of HC_6H^+

Calculated vertical excitation energies (ΔE_e), corresponding oscillator strengths (f), and the configuration character for the doublet states of HC_6H^+, are given in Table 2. Inspection
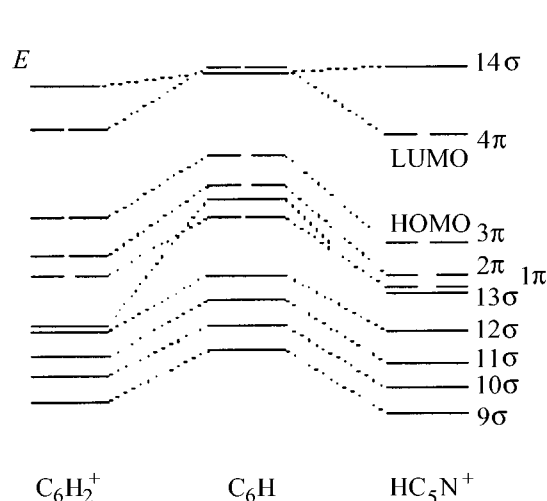

Fig. 1 Optimized geometries of isoelectronic species HC_6H^+, C_6H and HC_5N^+ at various levels of theory.

Table 1 Vibrational frequencies of isoelectronic species $C_6H_2{}^+$, C_6H and HC_5N^+

	$C_6H_2{}^+$		C_6H		HC_5N^+	
	Calc.	Expt.[a]	Calc.	Expt.	Calc.	Expt.[b]
$v_1(\sigma)$	3403	3313				
$v_2(\sigma)$	3401	3328	3457		3381	3403
$v_3(\sigma)$	2264	2201	2137	2202[c]	2278	2194
$v_4(\sigma)$	2112	2125	2105	1962[d]	2156	2070
$v_5(\sigma)$	1981	2019	1895		1998	1913
$v_6(\sigma)$	1266	1115	1224		1251	1213
$v_7(\sigma)$	656	625	650		643	625
$v_8(\pi)$	690	625				
$v_9(\pi)$	681	622	567		704	
$v_{10}(\pi)$	609	491	570		621	
$v_{11}(\pi)$	467	443	397		475	
$v_{12}(\pi)$	261	258	210		264	
$v_{13}(\pi)$	110	105	93		108	

[a] Ref 21. [b] Ref 7. [c] Ref 8. [d] Ref 22.

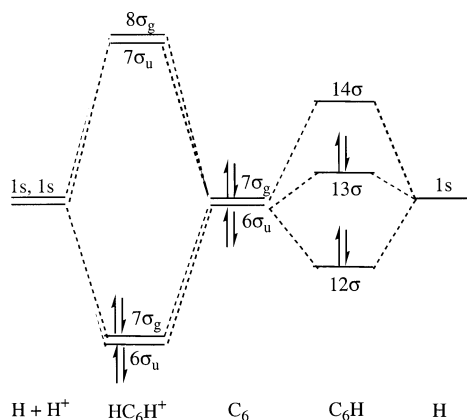**Fig. 2** Molecular orbital relative energies of HC_6H^+, C_6H and HC_5N^+.

Fig. 3 Energy levels of relevant orbitals in C_6, HC_6H^+ and C_6H and their mixing with hydrogens.

of the results in Table 2 immediately reveals that no low-lying electronic states due to σ electron promotion are found in the energy range up to approximately 6 eV. The excited state $1\,^2\Sigma_g^+$ due to the $7\sigma_g \to 2\pi_u$ excitation is calculated at 7.77 eV above the ground state $X\,^2\Pi_u$. This pattern can be understood from the qualitative arguments based on the stability of σ MOs as discussed above. The lowest transition of $X\,^2\Pi_u \to 1\,^2\Pi_g$, arising from the $1\pi_g \to 2\pi_u$ excitation, occurs at 2.22 eV ($f = 0.058$). This value is in agreement with the observed band at 2.05 eV.[5] The next $2\pi_u \to 2\pi_g$ excitation, *i.e.* HOMO–LUMO electron promotion, results in the excited states $2\,^2\Pi_g$, $1\,^2\Phi_g$ and $3\,^2\Pi_g$ at 3.58, 4.01 and 4.54 eV, respectively. Corresponding $X\,^2\Pi_u \to 2\,^2\Pi_g$ and $X\,^2\Pi_u \to 3\,^2\Pi_g$ transitions have oscillator strengths of 0.017 and 0.012, respectively, and they should be observable experimentally. The forbidden $X\,^2\Pi_u \to 2\,^2\Pi_u$, $X\,^2\Pi_u \to 1\,^2\Phi_u$ and $X\,^2\Pi_u \to 3\,^2\Pi_u$ transitions were predicted to occur at 3.79, 5.48 and 6.28 eV, respectively. If only the extrapolated MRD-CI energies are taken here, the $1\,^2\Pi_g$, $2\,^2\Pi_g$ and $1\,^2\Phi_g$ are predicted at 2.32, 3.76 and 4.11 eV, respectively. They are higher than those with the Davidson correction by 0.1–0.18 eV. A similar performance of the Davidson correction for other low-lying states is noted.

Energies of doublet states of C_6H

Table 3 collects the calculated vertical transition energies and oscillator strengths for the doublet system of C_6H. In contrast to the situation of HC_6H^+, a variety of excited states are found below 6 eV. The first excited state $1\,^2\Sigma^+$ is only 0.22 eV above the ground state. A recent photoelectron spectroscopy study presents a term value of 0.18 eV for the $1\,^2\Sigma^+$ state.[8] Previous CASPT2 calculations by Sobolewski and Adamowicz[27] and RCCSD(T) calculations by Woon[20] found the low-lying $1\,^2\Sigma^+$ state to be at 0.25 and 0.11 eV, respectively.

Table 2 Vertical transition energies and oscillator strength for doublet system of linear $C_6H_2^+$

State	$\Delta E_e/eV$	Transition	f^a
$X\,^2\Pi_u$	0.0	$...2\pi_u^3$	
$1\,^2\Pi_g$	2.22(2.05)[b]	$1\pi_g \to 2\pi_u$	0.0582
$2\,^2\Pi_g$	3.58	$2\pi_u \to 2\pi_g$	0.0166
$2\,^2\Pi_u$	3.79	$1\pi_u \to 2\pi_u$	0
$1\,^2\Phi_g$	4.01	$2\pi_u \to 2\pi_g$	0
$3\,^2\Pi_g$	4.54	$2\pi_u \to 2\pi_g$	0.0115
$1\,^2\Phi_u$	5.48	$1\pi_g \to 2\pi_g$	0
$3\,^2\Pi_u$	6.28	$1\pi_g \to 2\pi_g$	0

[a] All f values are listed for one component of degenerate states. [b] Experimental value from ref. 5.

Table 3 Vertical transition energies and oscillator strength for doublet system of linear C_6H

State	$\Delta E_e/eV$	Transition	f
$X\,^2\Pi$	0.00	$...3\pi^3$	
$1\,^2\Sigma^+$	0.22(0.18)[a]	$13\sigma \to 3\pi$	0.0002
$2\,^2\Pi$	2.56(2.34)[b]	$2\pi \to 3\pi$	0.0222
$3\,^2\Pi$	3.43	$3\pi \to 4\pi$	0.0046
$1\,^2\Phi$	3.80	$3\pi \to 4\pi$	0
$2\,^2\Sigma^+$	3.84	$13\sigma 2\pi \to 3\pi 4\pi$	0.0053
		$13\sigma \to 4\pi$	
$4\,^2\Pi$	4.30	$3\pi \to 4\pi$	0.0024
$1\,^2\Sigma^-$	4.41	$13\sigma \to 4\pi$	0.0017
		$13\sigma 2\pi \to 3\pi 4\pi$	
$1\,^2\Delta$	4.53	$13\sigma \to 4\pi$	0.000 04
		$13\sigma 2\pi \to 3\pi 4\pi$	
$2\,^2\Sigma^-$	4.61	$13\sigma \to 4\pi$	0.0080
		$13\sigma 2\pi \to 3\pi 4\pi$	
$2\,^2\Delta$	4.72	$13\sigma \to 4\pi$	0.0074
		$13\sigma 2\pi \to 3\pi 4\pi$	
$3\,^2\Sigma^+$	5.73	$13\sigma \to 3\pi$	0.0095
		$13\sigma 2\pi \to 3\pi 4\pi$	

[a] Experimental value from ref. 8. [b] Experimental value from ref. 5.

The strongest $X\,^2\Pi \to 2\,^2\Pi$ transition, arising from the $2\pi \to 3\pi$ excitation, was predicted to occur at 2.56 eV. This calculated value agrees reasonably with the experimental value of 2.34 eV.[5] The $3\pi \to 4\pi$ electron excitation, *i.e.* HOMO–LUMO electron promotion, gives rise to the low-lying states $3\,^2\Pi$, $1\,^2\Phi$ and $4\,^2\Pi$ at 3.43, 3.80 and 4.30 eV, respectively. $X\,^2\Pi$–$^2\Pi$ systems of C_6H are comparable with those of HC_6H^+ in energy and oscillator strength. In this system states involving σ MO promotions are seen to occur in lower-energy range; the $13\sigma \to 4\pi$ excitation, along with contribution of the double $13\sigma\,2\pi \to 3\pi\,4\pi$ excitation, leads to a variety of $X\,^2\Pi$–$^2\Sigma^-$, $X\,^2\Pi$–$^2\Sigma^+$ and $X\,^2\Pi$–$^2\Delta$ systems in the range 3.84–5.73 eV. The $3\pi \to 14\sigma$ excitation has been found at higher energies in preliminary calculations and is therefore not considered here.

Energies of doublet states of HC_5N^+

Table 4 presents the vertical transition energies and oscillator strengths for the doublet states of HC_5N^+. Our calculations predict that a strong $X\,^2\Pi \to 2\,^2\Pi$ transition occurs at 2.17 eV ($f = 0.069$), which matches the observed band at 2.13 eV very well.[5,7] The next excited state $1\,^2\Sigma^+$ was found at 2.47 above the ground state. The $3\,^2\Pi$ state mainly contributed by the $1\pi \to 3\pi$ excitation is 3.57 eV higher than the ground state. The corresponding $X\,^2\Pi \to 3\,^2\Pi$ transition has an oscillator strength of 0.017. The excited states $4\,^2\Pi$ and $1\,^2\Phi$ arise from the $3\pi \to 4\pi$ excitation, *i.e.* HOMO–LUMO electron promotion. Both states are calculated at 3.59 and 4.06 eV, respectively. The $X\,^2\Pi \to 2\,^2\Sigma^+$ and $X\,^2\Pi \to 1\,^2\Delta$ transitions were predicted to take place at 5.82 ($f = 0.0037$) and 6.19 eV ($f = 0.0002$), respectively.

Table 4 Vertical transition energies and oscillator strength for doublet system of linear HC_5N^+

State	$\Delta E_e/eV$	Transition	f
$X\,^2\Pi$	0.00	$...3\pi^3$	
$2\,^2\Pi$	2.17(2.13)[a]	$2\pi \to 3\pi$	0.0687
$1\,^2\Sigma^+$	2.47	$13\sigma \to 3\pi$	0.0008
$3\,^2\Pi$	3.57	$1\pi \to 3\pi$	0.0166
$4\,^2\Pi$	3.59	$3\pi \to 4\pi$	0.0047
$1\,^2\Phi$	4.06	$3\pi \to 4\pi$	0
$2\,^2\Sigma^+$	5.82	$13\sigma \to 4\pi$	0.0037
$1\,^2\Delta$	6.19	$13\sigma \to 4\pi$	0.0002

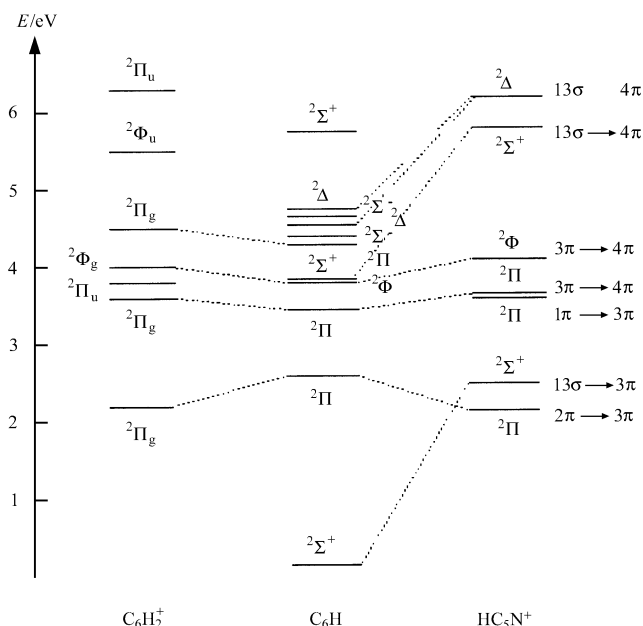[a] Experimental value from ref. 5 and 7.

E/eV

Fig. 4 Relative energies of the low-lying states in isoelectronic species HC_6H^+, C_6H and HC_5N^+.

Comparison of low-lying electronic states

The relative energies of relevant excited states of isoelectronic species HC_6H^+, C_6H and HC_5N^+ are depicted in Fig. 4. The relative energy pattern in Fig. 4 shows that only $^2\Pi$ and $^2\Phi$ excited states characterized by the π–π excitation are comparable in energy and oscillator strength among the isoelectronic species, while other low-lying electronic states such as $^2\Sigma$ and $^2\Delta$ series are significantly different among these isoelectronic species. These similarities and differences in energy for these low-lying states of isoelectronic species HC_6H^+, C_6H and HC_5N^+ can be understood to a certain extent from their distinct MO energy patterns. On the other hand, electron correlation plays also an essential role in determining the properties of the excited states of these carbon chains. For example, the $^2\Sigma^+$ low-lying states arising from the $13\sigma \rightarrow 3\pi$ excitation in C_6H and HC_5N^+ species should be comparable from the MO energy pattern point of view (see Fig. 2). However, a large shift to high excitation energy for the $^2\Sigma^+$ states of HC_5N^+ occurs due to difference in electron correlation of both species. There is a similar shift for the $^2\Delta$ state in HC_5N^+.

Summary and conclusions

B3LYP and extensive *ab initio* calculations on structures, harmonic vibrational frequencies and electronic spectra of isoelectronic species HC_6H^+, C_6H and HC_5N^+ have been performed. In comparison with the sophisticated *ab initio* calculations and available experimental results, B3LYP calculations reproduce reliably the geometrical parameters and harmonic vibrational frequencies for the ground states of these linear carbon chains. Bond lengths optimized at several levels of theory employed here reveal the main character of the acetylenic structure in the ground states of these species.

MRCI calculations predict that the strongest bands correspond to the $X\,^2\Pi \rightarrow 1\,^2\Pi$ transitions at 2.22, 2.56 and 2.17 eV, respectively, for the species HC_6H^+, C_6H and HC_5N^+. These calculated term energies, respectively, agree reasonably with observed bands at 2.05,[5] 2.34[5] and 2.17 eV.[5,7] Notable contributions of 1s orbitals from two H atoms in HC_6H^+ to the bonding of $7\sigma_g$ and $6\sigma_u$ MOs enlarge the splitting between $(7\sigma_g, 6\sigma_u)$ and $(8\sigma_g, 7\sigma_u)$ in comparison with neutral C_6, which make the transition due to σ electron promotion appear in the rather high energy region beyond 7 eV. A small energy difference of 0.22 eV between the first excited state $1\,^2\Sigma^+$ and the ground state $X\,^2\Pi$ in the species C_6H was found by MRCI calculations. This is similar to the situation in C_2H in which an interaction between the $^2\Pi$ and $^2\Sigma^+$ states dominates the low-energy vibronic spectra.[28] For HC_5N^+, the energy levels of $^2\Sigma$ and $^2\Delta$ series due to the $13\sigma \rightarrow 3\pi$ excitation have significant shifts towards higher energies compared to corresponding electronic states in C_6H.

Acknowledgement

References

1 J. H. Kiefer, S. S. Sidhu, R. D. Kern, K. Xie, H. Chen and L. B. Harding, *Combust. Sci. Technol.*, 1992, **82**, 101.
2 J. Cernicharo and M. Guelin, *Astron. Astrophys.*, 1996, **309**, L27.
3 J. Fulara, D. Lessen, P. Freivogel and J. P. Maier, *Nature*, 1993, **366**, 439.
4 C. Kirby, H. W. Kroto and D. R. M. Walton, *J. Mol. Spectrosc.*, 1980, **83**, 261.
5 (a) J. P. Maier, *Chem. Soc. Rev.*, 1997, 21; (b) J. P. Maier, *J. Phys. Chem. A*, 1998, **102**, 3462.
6 D. A. Kirkwood, M. Tulej, M. V. Pachkov, M. Schnaiter, F. Güthe, M. Grutter, M. Wyss and J. P. Maier, *J. Chem. Phys.*, 1999, **111**, 9280.
7 A. M. Smith, J. Agreiter and V. E. Bondybey, *Chem. Phys. Lett.*, 1995, **244**, 379.
8 T. R. Taylor, C. Xu and D. M. Neumark, *J. Chem. Phys.*, 1998, **108**, 10018.
9 A. D. Becke, *J. Chem. Phys.*, 1993, **98**, 5648.
10 C. Lee, W. Yang and R. G. Parr, *Phys. Rev. B*, 1988, **37**, 785.
11 A. D. Mclean and G. S. Chandler, *J. Chem. Phys.*, 1980, **72**, 5639.
12 R. Krishnan, J. S. Blinkley, R. Seeger and J. A. Pople, *J. Chem. Phys.*, 1980, **72**, 650.
13 T. H. Dunning, Jr., *J. Chem. Phys.*, 1989, **90**, 1007.
14 M. J. Frisch *et al.*, *GAUSSIAN 94, Revision B.3*, Gaussian Inc, Pittsburgh, PA, 1994.
15 H.-J. Werner *et al.*, *MOLPRO*; see www.tc.bham.ac.uk/molpro.
16 P. Poirier, R. Kari and I. G. Csizmadia, *Handbook of Gaussian Basis Sets*, Elsevier, Amsterdam, 1985.
17 M. Hanranth and B. Engels, *Chem. Phys.*, 1997, **225**, 167.
18 Z. Cao and S. D. Peyerimhoff, *J. Phys. Chem.*, A, 2000, **105**, 627.
19 R. J. Buenker and S. D. Peyerimhoff, in *New Horizons of Quantum Chemistry*, ed. P. O. Löwdin and B. Pullman, Reidel, Dordrecht, 1983.
20 (a) D. E. Woon, *Chem. Phys. Lett.*, 1995, **244**, 45; (b) W. E. Sinclair, D. Pfluger, H. Linnartz and J. P. Maier, *J. Chem. Phys.*, 1999, **110**, 296; (c) J. C. Pearson, C. A. Gottlieb, D. R. Woodward and P. Thaddeus, *Astron. Astrophys.*, 1988, **189**, L13; (d) W. E. Sinclair, D. Pfluger and J. P. Maier, *J. Chem. Phys.*, 1999, **111**, 9600.
21 M. Allan, E. Kloster-Jensen and J. P. Maier, *Chem. Phys.*, 1976, **17**, 11.
22 D. Forney, J. Fulara, P. Freivogel, M. Jakobi, D. Lessen and J. P. Maier, *J. Chem. Phys.*, 1995, **103**, 48.
23 J. Hutter, H. P. Lüthi and F. Diederich, *J. Am. Chem. Soc.*, 1994, **116**, 750.
24 J. M. L. Martin, J. El-Yazal and J. P. François, *Chem. Phys. Lett.*, 1995, **242**, 570.
25 S. T. Brown and J. C. Rienstra-Kiracofe and H. F. Schaefer, III, *J. Phys. Chem. A*, 1999, **103**, 4065.
26 R. J. Buenker, S. D. Peyerimhoff and J. L. Whitten, *J. Chem. Phys.*, 1967, **46**, 2029.
27 A. L. Sobolewski and L. Adamowicz, *J. Chem. Phys.*, 1995, **102**, 394.
28 M. Peric, S. D. Peyerimhoff and R. J. Buenker, *Z. Phys. D*, 1992, **24**, 177.